

Strategies for the Improvement of the Hydrogen Storage Properties of Metal Hydride Materials

Hui Wu^{*[a, b]}

Metal hydrides are an important family of materials that can potentially be used for safe, efficient and reversible on-board hydrogen storage. Light-weight metal hydrides in particular have attracted intense interest due to their high hydrogen density. However, most of these hydrides have rather slow absorption kinetics, relatively high thermal stability, and/or problems with the reversibility of hydrogen absorption/desorption cycling. This paper dis-

cusses a number of different approaches for the improvement of the hydrogen storage properties of these materials, with emphasis on recent research on tuning the ionic mobility in mixed hydrides. This concept opens a promising pathway to accelerate hydrogenation kinetics, reduce the activation energy for hydrogen release, and minimize deleterious possible by-products often associated with complex hydride systems.

1. Introduction

Hydrogen, as an energy carrier, can in principle be produced from a diverse range of sources. It is also a clean fuel, and forms water as a non-polluting by-product during use.^[1] Therefore, successful development of hydrogen as a primary fuel could simultaneously reduce dependence on fossil fuel and emissions of greenhouse gases and pollutants. This is especially critical in this century given increasing concerns about energy security and global warming. Extensive efforts are being made to develop a sustainable hydrogen economy in terms of production, delivery, storage, and fuel cells (including combustion engines in vehicles and stationary/portable power applications).^[2] Regarding hydrogen storage, advanced tank systems with purely physical hydrogen storage in gaseous and liquid form have been engineered and utilized in some fuel-cell vehicles.^[3] However, compared to pressurised gaseous or cryogenically liquefied hydrogen, storing hydrogen in solid state materials has definite advantages with regard to gravimetric and volumetric density, safety, and energy efficiency. One of the major challenges to widespread use of hydrogen is the lack of suitable hydrogen storage materials with on-board operating storage capabilities for fuel-cell vehicular applications.^[1,2,4] Current hydrogen storage materials under intense investigation include metal hydrides, chemical hydrides and high-surface-area adsorbents, which can store hydrogen chemically or physically in the form of atoms, ions or molecules.^[1,2]

In the context of metal hydrides, which include conventional (e.g. LaNi_5H_6 , Mg_2NiH_4) and complex hydrides (e.g. alanates, borohydrides, and amides),^[5] extensive interest has been focused on the light-weight hydrides (e.g. LiH , MgH_2 , LiBH_4 , and LiNH_2) due to their high gravimetric and volumetric hydrogen densities. However, all known hydrides have one or more limitations for on-board storage applications: 1) relatively high thermal stability, 2) slow desorption/absorption kinetics, 3) undesirable by-product gases (e.g. ammonia), and 4) irreversibility on cycling.^[2,4] Herein, we discuss different approaches for the improvement of hydrogen storage properties of metal hydride

materials, with emphasis on strategies which improve the absorption/desorption kinetics, reduce the operating temperatures, and/or improve the purity of the desorbed hydrogen gas.

2. Hydride Destabilization

Strongly bound light-weight hydrides, for example, alkali or alkaline earth metal hydrides or complex hydrides, are challenging for hydrogen storage mostly because their stability is too high for dehydrogenation/hydrogenation to be achieved at practical pressures and temperatures.^[4,5] For example, LiH contains 12.5 wt% hydrogen, but has a dehydrogenation enthalpy of $190 \text{ kJ mol}^{-1} \text{ H}_2$, and it requires a desorption temperature of 910°C at an equilibrium pressure of 1 bar.^[6] An approach to altering the hydrogenation/dehydrogenation thermodynamics of the stable light-weight hydrides is to destabilize them through alloy formation upon dehydrogenation by adding alloying additives.^[7,8] If the cohesive energy of the alloy formed between the additives and the dehydrogenated metal is large, the system then can be cycled between the hydride and the alloy compound instead of the elemental metal. In such a way, the dehydrogenation enthalpy of the system, and thereby the desorption temperature, is lowered significantly. As an example, we discuss the positive effect of alloying lithium hydride with silicon.

[a] H. Wu
Department of Materials Science and Engineering
University of Maryland
College Park, MD 20742-2115 (USA)

[b] H. Wu
NIST Center for Neutron Research
National Institute of Standards and Technology
Gaithersburg, MD, 20899-6102 (USA)
Fax: (+1) 301-975-9847
E-mail: huiwu@nist.gov

Si, a relatively light-weight semi-metal, can destabilize alkali and alkaline-earth metal hydrides such as LiH, MgH_2 ^[8] and CaH_2 ^[9] as it can easily form stable compounds with these light metals. For LiH, upon the formation of various Li_xSi_y alloys (e.g. LiSi, $\text{Li}_{12}\text{Si}_7$, Li_7Si_3 , $\text{Li}_{13}\text{Si}_4$, and $\text{Li}_{22}\text{Si}_5$), the dehydrogenation enthalpies are lowered to approximately $120 \text{ kJ mol}^{-1} \text{ H}_2$ and the desorption temperatures at 1 bar equilibrium pressure are reduced to 470°C .^[8] This is schematically shown in Figure 1.

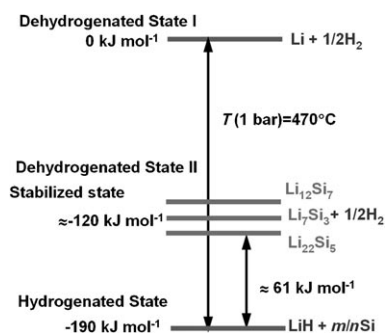


Figure 1. Modification of thermodynamics of the destabilized LiH/Si system (adapted from refs. [7] and [8]). The energy of the strongly bound LiH can be lowered considerably through the formation of Li_xSi_y intermetallics upon addition of Si. Hydrogenation/dehydrogenation then occurs between LiH/Si and Li_xSi_y instead of between pure Li and LiH.

However, with the added weight of the additional Si, the H_2 stored in the system is decreased to 2.8–7 wt%, lower than for pure LiH. In some cases with a particular ratio of LiH and Si, a new ternary hydride $\text{Li}_4\text{Si}_2\text{H}$ is formed that has relatively high stability after rehydrogenation (as also found for $\text{Li}_4\text{Ge}_2\text{H}$).^[8,10] The existence of this stable ternary phase changes the thermodynamic scheme of the original destabilization system, and thus leads to an incomplete dehydrogenation afterward and a reduced cycling hydrogen content.

MgH_2 and CaH_2 can also be destabilized by Si through the formation of Mg_2Si for the MgH_2/Si system,^[8] and CaSi, Ca_2Si or Ca_5Si_3 for CaH_2/Si .^[9] However, the kinetics of MgH_2 is too slow to achieve the rehydrogenation of Mg_2Si at practical pressures and temperatures. The three Ca–Si alloys can all be recycled with different hydrogenation characteristics. In particular, the formation of an amorphous hydride upon hydrogenation of Ca_2Si largely accelerates the absorption rate,^[9b] and it can be reformed through recycling. The role of amorphization in absorption kinetics is of significant interest and is also relevant for the development of robust H_2 purification membranes, and thus has stimulated more experimental and theoretical work.^[11]

3. Catalytic Additives

Since the important work of Bogdanovic and Schwickardi on TiCl_3 doped NaAlH_4 ,^[12] catalytic doping has stimulated great interest in the improvement of the kinetics of light metal hydrides and complex hydrides. Numerous hydrides with a variety of catalysts have been screened both theoretically and experimentally, and some catalytic additives have been reported

to improve the kinetics of the hydride systems effectively by reducing the activation barrier for diffusion and facilitating hydrogen dissociation.

A notable example is TiCl_3 , which substantially improves the kinetics and the reversibility of NaAlH_4 with a total hydrogen storage capacity of 5.6 wt%.^[12] NaAlH_4 stores H_2 reversibly via a two-step reaction, and catalyst doping allows hydrogen to be released at 120 and 175°C at 1 bar equilibrium pressure.^[5,13] The catalytic mechanism of TiCl_3 on hydrogen uptake and release in NaAlH_4 still remains uncertain, although numerous experimental and theoretical efforts have been made to study the distribution of Ti in the hydrides and to understand its effect.^[14] The only firmly established fact from these studies is the location of Ti, which is mostly located in the Al phase.^[14] Appealing defect- or vacancy-mediated dehydrogenation mechanisms have recently been proposed.^[14e,f] Another example of the utility of catalysts is Nb_2O_5 doped MgH_2 . The sluggish sorption kinetics of MgH_2 can be increased dramatically to 7 wt% of reversible hydrogen at 250°C and a lowering of the activation energy to $61 \text{ kJ mol}^{-1} \text{ H}_2$.^[15]

Besides the conventional transition-metal-based catalysts, new strategies for formation of new hydride compounds have been devised, which induce both kinetic and thermodynamic enhancement. A study of the $\text{LiBH}_4\text{--LiNH}_2\text{--MgH}_2$ system^[16] showed that the intermediate compound $\text{Li}_2\text{Mg}(\text{NH})_2$ can behave as a nucleus for the subsequent reaction, leading to an enhancement of the overall kinetic properties through a self-catalyzing mechanism. In fact, the thermodynamics of the system is modified by coupled self-catalyzing reactions upon formation of the intermediate product.

4. Size Effects

Materials particles with small sizes often display modified physical behavior compared to the bulk. Reducing the particle size of the metal hydride to the nanometer range can result in enhanced kinetics, and in some cases, modified thermodynamics. Metal hydride nanoparticle or nanocomposites are usually prepared by high-energy ball milling. However, as it is difficult to control the particle size when milling is used, the size distribution is broad and the smallest particle size achievable is limited to $\sim 100 \text{ nm}$.^[17] This is usually inadequate to produce a dramatic size effect.

Alternative synthetic approaches have been adopted to prepare nanoscale hydrides and study size effects. For example, Mg nanowires, with the smallest diameters in the 30–50 nm range, were prepared using vapor-transport methods.^[18] The activation energy of hydriding/dehydriding for Mg in this scale is reduced to $34/39 \text{ kJ mol}^{-1} \text{ H}_2$, and the dehydrogenation enthalpy of hydrided nanowire is about $65.3 \text{ kJ mol}^{-1} \text{ H}_2$, smaller than bulk MgH_2 ($74 \text{ kJ mol}^{-1} \text{ H}_2$).^[18] However, with extended cycling, the nanowires tend to collapse into particles, and the kinetic enhancement diminishes, as these particles lose their nanostructure upon grain coarsening. A good approach for preserving the nanoscale dimension through hydriding/dehydriding cycles is to infiltrate the hydride materials into nanoporous scaffolds. This approach has been demonstrated in nano-

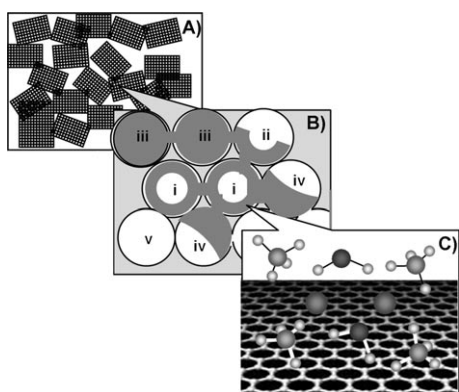


Figure 2. Overview of ways to reduce particle size of hydrides in nanoscaffold materials. A) Hydride infiltrated in nanoscaffolds, B) schematic of possible distributions of hydrides in nanopores: i) fully and ii) half-coating the surface of the pore; iii) fully and iv) half-filling the pores; v) closed pore without hydride infiltration; C) schematic of the interaction between a hydride and the wall of the pore that may affect the desorption process

scaffolded BH_3NH_3 ,^[19] LiBH_4 ,^[20] and $\text{Li}_3\text{BN}_2\text{H}_8$ (Figure 2),^[21] as well as in NaAlH_4 supported by porous carbon nanofibers,^[22] with particle sizes as low as 2 nm. The reduced particle size in all cases has been shown to lower the activation energy for the loss of H_2 significantly, modify the enthalpy of the dehydrogenation (lowered desorption temperature) effectively, and in some case, achieve reversibility and/or suppress the release of byproduct gases.

The enforced nanostructural geometry of the hydride materials confined in the scaffold matrix is expected to introduce a large number of defects. Certain interactions between the M–H bond and the wall of the nanopores may also catalyze the desorption process. Both effects would promote dehydrogenation at lower temperatures. In addition, the hydride distribution and filtration percentage are key factors. For example, if the hydrides are completely wetting the surface of the nanopores the nature of the hydrogen desorption will be different than if they are largely confined to the center of the pores. Although the detailed desorption mechanism of such nanoporous infiltration systems is complex, it is expected that hydrides in supporting materials with larger surface area and smaller pore size should achieve better storage and release performance. Nanopore size effects can also be complex. For example, it was recently reported that LiBH_4 in carbon aerogels with 4 nm average pore sizes actually show degraded desorption kinetics compared to those with a 13 nm pore size.^[23] Apparently, compared to the simple nanoparticle system, other factors such as hydride filtration percentage and distribution, the pore geometry of the scaffold materials, and even gas diffusion paths, can also affect the overall storage properties of the infiltration systems (see Figure 2b). Finally, the weight penalty of the supporting substrates reduces the system hydrogen storage capacity.

5. Tuning Small Ion Mobility

Recently, the binary mixtures $\text{LiNH}_2/\text{MgH}_2$,^[24] $\text{Mg}(\text{NH}_2)_2/\text{LiH}$,^[25] $\text{LiBH}_4/\text{LiNH}_2$,^[26] and $\text{LiBH}_4/\text{MgH}_2$ ^[27] have been shown to have

improved storage properties compared to their constituent compounds. However, these improvements are mainly caused by better dehydrogenation thermodynamics in terms of hydride destabilization via the formation of stable compounds, for example, MgB_2 ^[27] and Li_3BN_2 .^[26] The hydrogen mobility in these systems is not promoted. Therefore, the dehydrogenation kinetics of these systems is not really optimized and correlated with their equilibrium thermodynamic phase diagram. As a result, without tuning the reaction kinetics, the dehydrogenation reactions often do not occur within the desired thermodynamically stable regions. For example, the desorption path and the reversibility of $\text{LiBH}_4/\text{MgH}_2$ rely on the amount and the variety of catalysts.^[27] The observed desorption temperature of a $\text{LiH}/\text{Mg}(\text{NH}_2)_2$ mixture ($> 210^\circ\text{C}$) is much higher than the theoretically expected temperature (90°C at 1 bar H_2 pressure) derived from the measured dehydrogenation enthalpy and entropy.^[25] Besides, the purity of hydrogen desorbed in $\text{LiNH}_2/\text{MgH}_2$ and $\text{Mg}(\text{NH}_2)_2/\text{LiH}$ also depends on the operating temperatures.^[24] Therefore, the rational design of a hydrogen storage system must also depend on the interactions between thermodynamics of the system and the promoted kinetics.

Mobile interstitial ions and/or vacancies have been well studied in oxide electrolyte materials with a variety of structures such as perovskites, fluorites, melilites, etc.^[28] Either cations or anions can be the mobile species. Regarding hydrogen storage applications, hydride materials need higher thermal activation for dehydrogenation/hydrogenation due to the slow kinetics. Therefore, to accelerate the kinetics of the hydrogen storage systems, it is of considerable interest to learn from well-established oxide electrolyte systems, and introduce the structural characteristics of these fast ionic conductors to the metal hydride systems. Hydrogen in metal hydrides exists in the form of both H^- (e.g. LiH , MgH_2 , LiBH_4) and H^+ (e.g. LiNH_2 , Li_2NH). Because of the large difference in the first ionization energy, $I_p = 1312 \text{ kJ mol}^{-1}$ (13.60 eV), and electron affinity, $E_A = 72.8 \text{ kJ mol}^{-1}$ (0.75 meV), of a H atom,^[4] the conversion from the H^- anion with loosely held valence electrons to neutral H is much easier than that from H^+ or H^+ containing strongly bound complex ions. In general, it is better to involve H^- containing hydrides with relatively fast H^- motions for facile dehydrogenation.

One structural type that might accelerate hydrogen mobility is perovskite. Perovskite oxides are a well-established class of compounds that exhibit oxygen ionic conductivity, and can even be used as proton conductors.^[29] For example, NaMgH_3 shows reversible hydrogen storage properties.^[30] More importantly, its perovskite structure enables the rapid motion of hydrogen at high temperature,^[31] thus making it an intriguing material both for storing hydrogen and for facilitating kinetics modifications in the related hydride systems. NMR studies have shown that the hydrogen mobility in NaMgH_3 is orders of magnitude higher than that of MgH_2 , resulting in greatly enhanced absorption rates during hydrogenation.^[32] Although MgH_2 can be destabilized by Si, the resultant Mg_2Si is difficult to rehydride due to the kinetic limitations of MgH_2 . Our recent study showed that the hydrogenation properties of Mg_2Si can effectively be improved via the formation of NaMgH_3 instead

of MgH_2 by the addition of Na to Mg_2Si .^[31] The heat of formation of NaMgH_3 ($-96 \text{ kJ mol}^{-1} \text{ H}_2$) is much larger than that of MgH_2 ($-76.15 \text{ kJ mol}^{-1} \text{ H}_2$). Therefore, the formation of NaMgH_3 actually modifies both the thermodynamics and kinetics, and renders Mg_2Si more able to form hydrides.

Besides the mobility of hydrogen, other small ion species in hydrides may also play an important role in facilitating hydrogenation/dehydrogenation properties. For example, materials with fluorite structures are well known for their high conductivity. Compared to the fast ionic fluorites, such as UO_{2+x} ,^[33] Li_2O forms an antifluorite structure, where the position of cations and anions are reversed. Therefore it is cations that are mobile and fast Li^+ migration among different sites has been observed in the structure at elevated temperatures.^[34] Li_2NH adopts the same structure as Li_2O , and LiNH_2 has a closely related structure. Indeed, structural studies of $\text{LiNH}_2/\text{Li}_2\text{NH}$ showed rapid motion of Li^+ at high temperatures during dehydrogenation, resulting in a series of non-stoichiometric $\text{Li}_{2-x}\text{NH}_{1+x}$ and $\text{Li}_{1+x}\text{NH}_{2-x}$ compounds.^[35]

These results suggest that, without the aid of catalysts, the reaction kinetics can still be enhanced, inducing mobility for both cations and anions in compounds with special structure types. For example, we have demonstrated recently^[36] that a mixture of $\text{LiNH}_2/\text{CaH}_2$ shows significantly accelerated dehydrogenation/hydrogenation with much lower desorption/absorption temperatures than the constituent LiNH_2 and CaH_2 , as illustrated in Figure 3. Similar to $\text{LiNH}_2/\text{MgH}_2$, the dehydrogenation thermodynamics of $\text{LiNH}_2/\text{CaH}_2$ is enhanced due to the very high enthalpy of the H^- and H^+ combination reaction [$\Delta H = -1676 \text{ kJ mol}^{-1} \text{ H}_2$ (-17.37 eV)].^[4] While different from the slow hydrogen diffusion in MgH_2 , H^- ions are highly mobile in CaH_2 due to the presence of a small amount of hydrogenation vacancies at the elevated temperatures. The fast-moving H^- ions in CaH_2 rapidly combine with H^+ in LiNH_2 and release H_2 . Such a fast reaction also leaves the oppositely charged anion vacancies and cation vacancies in the mixture and drives the reaction of these two defects on the surface of adjacent LiNH_2 and CaH_2 particles. Another significant effect of CaH_2 is that the highly mobile H^- ions consume most of the H^+ in LiNH_2 , thus preventing the backflow of H^+ into the lithium vacancies ($[\square_{\text{Li}}\text{NH}_2]^-$), which are generated by the hopping of Li^+ ions in LiNH_2 , thereby minimizing the formation of ammonia. Therefore, by tuning the ionic mobility of the metal hydride, the reaction kinetics and the thermodynamics can be correlated so that the dehydrogenation occurs along a more favorable reaction pathway.

We also noticed that the dehydrogenation product $\text{Li}_2\text{Ca}(\text{NH})_2$ adopts a layered structure consisting of infinite 2D slabs of edge-shared $\text{Ca}(\text{NH})_6$ octahedra separated by the motif of Li cations. The heavier Ca cations and the strongly covalent bonded NH_2^- group in the CaNH layers are relatively inert, while the Li cation confined in these 2D channels are quite mobile, which is confirmed by the increasing nonstoichiometry at Li lattice sites at elevated temperatures revealed by our structural study (see Figure 3).^[36] The facile motion of these small species in the channels generates Li_i^+ interstitials and Li vacancies ($[\square_{\text{Li}}\text{LiNH}]^-$), which rapidly react with hydrogen gas

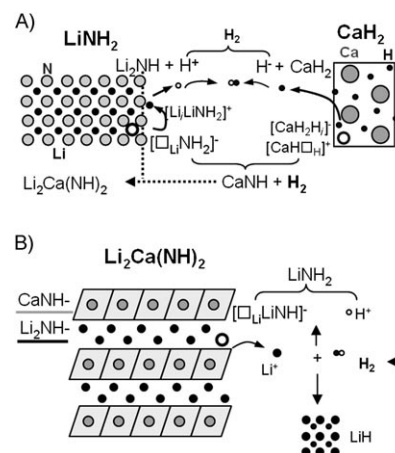


Figure 3. A) Schematic representation of the motion of Li^+ in LiNH_2 and H^- in CaH_2 facilitating the hydrogen desorption of the $\text{LiNH}_2/\text{CaH}_2$ mixture. Hopping of Li from the lattice sites in LiNH_2 creates charged interstitial ($\text{Li}_i\text{LiNH}_2^+$) and lithium vacancies ($[\square_{\text{Li}}\text{NH}_2]^-$); the charge balance can be restored by the recombination of the defect pair, or by a subsequent motion of Li^+ or H^+ . Anion interstitial (CaH_2H^-) and vacancy ($\text{CaH}[\square_{\text{H}}]^+$) can also be created in CaH_2 by H hopping from the anion lattice sites. The highly mobile H^- anion in CaH_2 and protonic H^+ in LiNH_2 can easily combine to create H_2 . The fast combination of H^+ and H^- leaves $[\square_{\text{Li}}\text{NH}_2]^-$ and $\text{CaH}[\square_{\text{H}}]^+$ in LiNH_2 and CaH_2 , and drives the reaction between these two defects, releasing another H_2 molecule. With further release of H_2 , all CaH_2 converts to CaNH , which reacts with Li_2NH to form $\text{Li}_2\text{Ca}(\text{NH})_2$. B) Schematic representation of the motion of Li along the 2D channels in promoting the hydrogen absorption of $\text{Li}_2\text{Ca}(\text{NH})_2$ with layered structure. $\text{Li}_2\text{Ca}(\text{NH})_2$ can be viewed as a combined structure with alternating Li_2NH and CaNH layers. In the layer of Li_2NH , mobile Li produces Li^+ interstitials and Li^- vacancies ($[\square_{\text{Li}}\text{LiNH}]^-$). The Li^+ reacts rapidly with hydrogen gas, forming LiH and a proton. The proton produced will then react with the negatively charged Li vacancy and form an amide group. In the layers of CaNH , covalently bonded H in NH^- groups and heavy Ca^{2+} cations are inert, so CaNH remains.

during hydrogenation, forming LiH and H^+ . The latter then easily react with oppositely charged Li vacancies and produce LiNH_2 . The rapid Li motion in such “intercalated” structures drives the hydrogenation kinetics, and these structural characteristics are mainly responsible for the dramatically lowered hydrogenation temperature.

Thus, in this system, the movement of small ionic species such as Li^+ , H^- , and H^+ has been shown to be the key process in hydrogenation and dehydrogenation. The major benefit of the participation of H^- is the enhanced interaction between H^- and H^+ that allows hydrogen to be released at lower temperatures and reduces the interaction between H^+ and NH_2^- , which produces unwanted ammonia. This process also drives the subsequent interactions between the other positively and negatively charged species. Moreover, the resultant ternary imide with a layered structure allows rapid Li^+ ionic movement, leading to a much lower hydrogen absorption temperature in comparison to Li_2NH . Therefore, the differently charged small mobile species are primarily responsible for the reduced dehydrogenation/hydrogenation temperatures and for the minimized ammonia release in the mixed amide/hydride system.

Beyond $\text{LiNH}_2/\text{CaH}_2$, the approach of tuning ionic mobility to facilitate the reaction kinetics can be applied generally. As

demonstrated herein, we can design and form certain crystal structures with facile ionic immigration pathways such as perovskite NaMgH_3 and layered $\text{Li}_2\text{Ca}(\text{NH})_2$. Another effective way to enhance ionic mobility is to increase the concentration of vacancies or small ionic species in the structure through doping, nonstoichiometries, and defects. Moreover, certain crystal structures with a large concentration of intrinsic structural vacancies that usually exhibit dramatic ionic conductivity may also be used as prototypes to design and prepare new hydrogen storage materials. Finally, the decrease of diffusion distances is also known to facilitate significantly the migration of small ions. Therefore, engineering the size of material particles can be also used to tune the ionic mobility, and thus dramatically benefit the absorption and desorption performance.

6. Conclusions

Four approaches for improving the hydrogen storage properties of metal hydride materials are discussed herein, including hydride destabilization, catalysis, particle size reduction, and tuning small ion mobility. All these strategies have been shown to help overcome one or more limitations of current hydrogen storage materials, but thus far no modified materials can simultaneously meet all requirements for practical hydrogen storage applications. Among the options for improved performance, the tuning of small ion mobility has some advantages. This approach does not induce an added weight penalty, facilitate hydrogenation kinetics and dramatically reduce production of unwanted by products (e.g. NH_3). It is clear, however, that extensive research is needed to achieve high hydrogen capacity and convenient and safe storage of hydrogen in metal hydride materials.

Acknowledgements

I thank Dr. John Rush for his valuable comments on this paper. I have greatly benefited from collaborations and other interaction with Dr. John Rush, Dr. Terrence Udovic, Dr. Wei Zhou, Dr. Taner Yildirim, Dr. Michael Hartman, Dr. Robert Bowman Jr., and Dr. John Vajo. Some of our work described in this article is supported by the DOE through EERE Grant No. DE-AI-01-05EE11104.

Keywords: hydrides • hydrogen storage • hydrogenation/dehydrogenation • ionic mobility • kinetics

- [1] A. Zuttel, L. Schlapbach, *Nature* **2001**, *414*, 353–358.
- [2] <http://www.hydrogen.energy.gov/>.
- [3] R. von Helmolt, U. Eberle, *J. Power Sources* **2007**, *165*, 833–843.
- [4] W. Grochala, P. P. Edwards, *Chem. Rev.* **2004**, *104*, 1283–1315.
- [5] a) F. Schüth, B. Bogdanovic, M. Felderhof, *Chem. Commun.* **2004**, *37*, 2249–2258; b) S. Orimo, Y. Nakamori, J. R. Eliseo, A. Zuttel, C. M. Jensen, *Chem. Rev.* **2007**, *107*, 4111–4132.
- [6] J. Sangster, A. D. Pelton in *Phase Diagrams of Binary Hydrogen Alloys*; (Ed.: F. D. Manchester), ASM International, Materials Park, **2000**, pp. 74.
- [7] J. J. Vajo, G. L. Olsen, *Scr. Mater.* **2007**, *56*, 829–834.
- [8] a) J. J. Vajo, F. Mertens, C. C. Ahn, R. C. Bowman, Jr., B. J. Fultz, *J. Phys. Chem. B* **2004**, *108*, 13977–13983; b) R. C. Bowman, Jr., S.-J. Hwang, C. C. Ahn, J. J. Vajo, *Mater. Res. Soc. Symp. Proc.* **2005**, *837*, 3.6.1–3.6.6.
- [9] a) H. Wu, W. Zhou, T. J. Udovic, J. J. Rush, T. Yildirim, *Phys. Rev. B* **2006**, *74*, 224101; b) H. Wu, W. Zhou, T. J. Udovic, J. J. Rush, *Chem. Mater.* **2007**, *19*, 329–334; c) H. Wu, W. Zhou, T. J. Udovic, J. J. Rush, T. Yildirim, *Chem. Phys. Lett.* **2008**, *460*, 432–437.
- [10] a) H. Wu, M. R. Hartman, T. J. Udovic, J. J. Rush, W. Zhou, R. C. Bowman, Jr., J. J. Vajo, *Acta Crystallogr. Sect. B* **2007**, *63*, 63–68; b) H. Wu, W. Zhou, T. J. Udovic, J. J. Rush, T. Yildirim, M. R. Hartman, R. C. Bowman, Jr., J. J. Vajo, *Phys. Rev. B* **2007**, *76*, 224301.
- [11] S. Hao, M. Widom, D. S. Sholl, private communication.
- [12] B. Bogdanovic, M. Schwickardi, *J. Alloys Compd.* **1997**, *253*, 1–9.
- [13] B. Bogdanovic, U. Eberle, M. Felderhoff, F. Schuth, *Scr. Mater.* **2007**, *56*, 813–816.
- [14] a) X. D. Kang, P. Wang, H. M. Cheng, *J. Appl. Phys.* **2006**, *100*, 034914; b) O. M. Løvvik, S. M. Opalka, *Appl. Phys. Lett.* **2006**, *88*, 161917; c) J. M. Bellosta von Colbe, W. Schmidt, M. Felderhoff, B. Bogdanovic, F. Schuth, *Angew. Chem.* **2006**, *118*, 3745–3747; *Angew. Chem. Int. Ed.* **2006**, *45*, 3663–3665; d) O. Palumbo, A. Paolone, R. Cantelli, C. M. Jensen, R. Ayabe, *Mat. Sci. Eng. A* **2006**, *442*, 75–78; e) A. Peles, C. G. Van de Walle, *Phys. Rev. B* **2007**, *76*, 214101; f) H. Gunaydin, K. N. Houk, V. Ozolins, *Proc. Natl. Acad. Sci. USA* **2008**, *105*, 3673–3677; g) O. M. Løvvik, S. M. Opalka, *Phys. Rev. B* **2005**, *71*, 054103; h) J. Íñiguez, T. Yildirim, T. J. Udovic, M. Sulic, C. M. Jensen, *Phys. Rev. B* **2004**, *70*, 060101.
- [15] G. Barkhordarian, T. Klassen, R. Bormann, *J. Alloys Compd.* **2004**, *364*, 242–246.
- [16] J. Yang, A. Sudik, D. J. Siegel, D. Halliday, A. Drews, R. O. Carter III, C. Wolverton, G. J. Lewis, J. W. A. Sachtler, J. J. Low, S. A. Faheem, D. A. Lesch, V. Ozolins, *Angew. Chem.* **2008**, *120*, 896–901; *Angew. Chem. Int. Ed.* **2008**, *47*, 882–887.
- [17] H. W. Brinks, B. C. Hauback, S. S. Srinivasan, C. M. Jensen, *J. Phys. Chem. B* **2005**, *109*, 15780–15785.
- [18] W. Li, C. Li, H. Ma, J. Chen, *J. Am. Chem. Soc.* **2007**, *129*, 6710–6711.
- [19] A. Gutowska, L. Li, Y. Shin, C. M. Wang, X. S. Li, J. C. Linehan, R. S. Smith, B. D. Kay, B. Schmid, W. Shaw, M. Gutowski, T. Autrey, *Angew. Chem.* **2005**, *117*, 3644–3648; *Angew. Chem. Int. Ed.* **2005**, *44*, 3578–3582.
- [20] A. F. Gross, J. J. Vajo, S. L. Atta, G. L. Olsen, *J. Phys. Chem. C* **2008**, *112*, 5651–5657.
- [21] H. Wu et al., *Nanotechnology*, unpublished results.
- [22] C. P. Baldé, B. P. C. Hereijgers, J. H. Bitter, K. P. de Jong, *J. Am. Chem. Soc.* **2008**, *130*, 6761–6765.
- [23] J. J. Vajo, P. Liu, present at DOE 2008 Annual Review, June 2008.
- [24] a) W. Luo, *J. Alloys Compd.* **2004**, *381*, 284–287; b) W. Luo, S. Sickafoose, *J. Alloys Compd.* **2006**, *407*, 274–281; c) Z. T. Xiong, G. T. Wu, J. J. Hu, P. Chen, *Adv. Mater.* **2004**, *16*, 1522–1525.
- [25] A. Sudik, J. Yang, D. Halliday, C. Wolverton, *J. Phys. Chem. C* **2007**, *111*, 6568–6573.
- [26] a) F. E. Pinkerton, G. P. Meisner, M. S. Meyer, M. P. Balogh, M. D. Kundrat, *J. Phys. Chem. B* **2005**, *109*, 6–8; b) G. P. Meisner, M. L. Scullin, M. P. Balogh, F. E. Pinkerton, M. S. Meyer, *J. Phys. Chem. B* **2006**, *110*, 4186–4192; c) H. Wu, W. Zhou, T. J. Udovic, J. J. Rush, T. Yildirim, *Chem. Mater.* **2008**, *20*, 1245–47.
- [27] a) J. J. Vajo, S. L. Skeith, F. Mertens, *J. Phys. Chem. B* **2005**, *109*, 3719; b) F. E. Pinkerton, M. S. Meyer, G. P. Meisner, M. P. Balogh, J. J. Vajo, *J. Phys. Chem. C* **2007**, *111*, 12881–12885.
- [28] X. Kuang, M. A. Green, H. Niu, P. Zajdel, C. Dickinson, J. B. Claridge, L. Jantsky, M. J. Rosseinsky, *Nat. Mater.* **2008**, *7*, 498–504.
- [29] a) M. Kajitani, M. Matsuda, A. Hoshikawa, S. Harjo, T. Kamiyama, T. Ishigaki, F. Izumi, M. Miyake, *Chem. Mater.* **2005**, *17*, 4235–4243; b) H. Hayaishi, H. Inaba, M. Matsuyama, N. G. Lan, M. Dokiya, H. Tagawa, *Solid State Ionics* **1999**, *122*, 1–15; c) P. R. Slater, J. T. S. Irvine, T. Ishihara, Y. Takita, *J. Solid State Chem.* **1998**, *139*, 135.
- [30] a) K. Ikeda, Y. Kogure, Y. Nakamori, S. Orimo, *Scripta Mater.* **2005**, *53*, 319–322; b) K. Ikeda, S. Kato, Y. Shinzato, N. Okuda, Y. Nakamori, A. Kitano, H. Yukawa, M. Morinaga, S. Orimo, *J. Alloy Compd.* **2007**, *446–447*, 162–165.
- [31] a) T. W. D. Farley, W. Hayes, S. Hull, M. T. Hutching, M. Vrtis, *J. Phys. Condens. Matter* **1991**, *3*, 4761–4781; b) M. Hayoun, M. Meyer, A. Denieport, *Acta Mater.* **2005**, *53*, 2867–2874.
- [32] H. Wu, W. Zhou, T. J. Udovic, J. J. Rush, T. Yildirim, *Chem. Mater.* **2008**, *20*, 2335–42.
- [33] M. Conradi, B. Corey, R. Bowman, Jr., R. Zidan, A. Stowe, private communication.

[34] G. C. Allen, P. A. Tempest, J. W. Tyler, *Nature* **1982**, 295, 48–49.

[35] W. I. F. David, M. O. Jones, D. H. Gregory, C. M. Jewell, S. R. Johnson, A. Walton, P. P. Edwards, *J. Am. Chem. Soc.* **2007**, 129, 1594–1601.

[36] H. Wu, *J. Am. Chem. Soc.* **2008**, 130, 6516–22.

Received: August 1, 2008

Published online on September 26, 2008
